Applied Catalysis B: Environmental 325 (2023) 122396

Contents lists available at ScienceDirect

Applied Catalysis B: Environmental

journal homepage: www.elsevier.com/locate/apcatb

New penta- and hexa-coordinated titanium sites in titanium silicalite-1 catalyst for propylene epoxidation

Yanli Wang [a], Hong Yang [b], Yi Zuo [a], Dongxu Tian [a], Guangjin Hou [c], Yaqiong Su [d], Zhaochi Feng [c,*], Xinwen Guo [a,*], Can Li [c,*]

[a] State Key Laboratory of Fine Chemicals, Frontier Science Center for Smart Materials, PSU-DUT Joint Center for Energy Research, School of Chemical Engineering, Dalian University of Technology, No.2 Linggong Road, Dalian 116024, China
[b] School of Engineering, The University of Western Australia, 35 Stirling Highway, Perth, WA 6009, Australia
[c] State Key Laboratory of Catalysis, Dalian Institute of Chemical Physics, Chinese Academy of Sciences, 457 Zhongshan Road, Dalian 116023, China
[d] School of Chemistry, Xi'an Key Laboratory of Sustainable Energy Materials Chemistry, State Key Laboratory of Electrical Insulation and Power Equipment, Xi'an Jiaotong University, Xi'an 710049, China

ARTICLE INFO

Keywords:
Titanium silicalite-1 catalyst
Propylene epoxidation
UV resonance Raman spectroscopy
Ti sites

ABSTRACT

Creating and identifying catalytically active titanium sites is vital to further enhance performance of titanium-containing zeolites, particularly for environmentally friendly titanium silicalite-1 catalyst (TS-1). Herein, we prepared a typical TS-1 with two new Ti-sites including the penta-coordinated $Ti(OH)_2(OSi)_3$ and hexa-coordinated $Ti(OH)_4(OSi)_2$. They are identified by UV resonance Raman spectroscopy and their coordination structures delineated by density functional theory calculations. Evaluated by propylene epoxidation to propylene oxide, $Ti(OH)_4(OSi)_2$ is more active than $Ti(OH)_2(OSi)_3$. Furthermore, $Ti(OH)_4(OSi)_2$ delivers the catalytic activity about 8.7 times the activity of known tetra-coordinated framework $Ti(OSi)_4$ sites. Thus, $Ti(OH)_4(OSi)_2$ is found to be highly active in this reaction.

1. Introduction

Titanium silicalite-1 (TS-1) is an MFI-type zeolite in which a small number of tetrahedral Si atoms are substituted by Ti in an otherwise purely siliceous framework [1]. It is an environmentally friendly catalyst which enables many oxidation reactions to be green processes, such as alkenes epoxidation, and ketones ammoximation, oxidation of alkanes and aromatics hydroxylation, all are using aqueous H_2O_2 solution as a mild and green oxidant [2–6].

Catalytic performance of TS-1 is the key to its application in these reactions and it is mainly determined by the catalytically active Ti-sites. So far, tetra-coordinated framework Ti site ("TiO_4"), tetra-coordinated dinuclear Ti site, hexa-coordinated Ti site ("$\ddot{T}iO_6$"), anatase-TiO_2 and amorphous Ti-O-Ti have been experimentally identified for the TS-1 [7–12]. A number of other Ti sites, including $NaTi(OSi)_5$ and $Na_2Ti(OSi)_6$ are also constructed by DFT calculations [13]. It is commonly believed that the "TiO_4" is the main active Ti-site for the pre-mentioned oxidation reactions [2–6,14,15]. However, the theoretical maximum amount of Ti in framework just accounts for 2.5 wt% in TS-1 [16]so that many efforts are made to enhance efficiency of "TiO_4" by improving diffusion conditions in TS-1.

Diffusion conditions are improved by decreasing particle size and/or generating hierarchical structures of TS-1 [17–23]. High surface energy in synthesis of extreme small TS-1 particles (<100 nm) and harsh separation processes restrict its further application [17,18]. Hierarchical structures are generated by using additives and/or introducing specific operations in hydrothermal processes. For hydrothermal synthesis, the second structure-directing agents (SDAs) are added to generate mesoporous or/and macroporous structure. For hydrothermal post-treatment of microporous TS-1, hierarchical structures are generated by leaching part of Si and Ti from TS-1 in alkaline solutions. SDAs, alkalis and salts are added to control the leaching process [19–23]. However, additives increase costs in TS-1 production and specific operations make preparation process more complex. More importantly, the leaching process and the competition between SDAs decrease "TiO_4" amount in TS-1. As a result, catalytic performance of TS-1 is difficult to be further enhanced by improving "TiO_4" efficiency, particularly to some specific reactions.

In this work, a pre-prepared TS-1 containing only "TiO_4" was post-treated by tetrapropylammonium hydroxide (TPAOH) aqueous solution, pre-hydrothermal treated TPAOH aqueous solution and mother

* Corresponding authors.
E-mail addresses: zcfeng@dicp.ac.cn (Z. Feng), guoxw@dlut.edu.cn (X. Guo), canli@dicp.ac.cn (C. Li).

https://doi.org/10.1016/j.apcatb.2023.122396
Received 3 November 2022; Received in revised form 17 December 2022; Accepted 9 January 2023
Available online 13 January 2023

liquor, respectively. Each of the post-treatment would break part of Ti-O-Si bonds in "TiO_4" and generated new bonds via a desilication-recrystallization process. New penta-coordinated and hexa-coordinated Ti sites were created by these processes and they were identified for the first time through detailed and systematic UV resonance Raman (UV-Raman) spectroscopy study coupled with DFT calculations. The new hexa-coordinated Ti site shows very high catalytic activity in propylene epoxidation to prepare propylene oxide.

2. Experimental

2.1. Material preparation

Microporous titanium silicalite-1 ($n(SiO_2)/n(TiO_2)$= 62) was hydrothermally synthesized. Ethyl orthosilicate, tetrapropylammonium hydroxide (TPAOH) and tetrabutyl titanate are silica source, template and titanium source, respectively. The hydrothermal synthesis was performed in Teflon-lined autoclave and held at 443 K under stirring for 72 h. The product was cooled down to room temperature and centrifugated. The solid product was dried at 373 K for 12 h and then calcined at 813 K for 6 h. This final product is the microporous m-TS-1. The remaining liquid product is named mother liquor (ML) which was collected for use in the post-treatment of m-TS-1.

TPAOH aqueous solution was transferred to a 100 ML Teflon-lined steel autoclave and held at 443 K for 72 h. After that, the autoclave was allowed to cool down to room temperature and the resulted product was labeled as TPAOH*. TPAOH aqueous solution, TPAOH* and mother liquor were used for hydrothermal post-treatment of m-TS-1, respectively. The hydrothermal post-treatment was performed in Teflon-lined autoclave and held at 443 K under stirring for 72 h. The product was cooled down to room temperature and centrifugated. The solid product was dried at 373 K for 12 h and then calcined at 813 K for 6 h. The final products are T-TS-1, T*-TS-1 and ML-TS-1, respectively.

A commercial anatase-TiO_2 was purchased from Sigma-Aldrich. Home-made TiO_2 was hydrothermally synthesized. TPAOH and tetrabutyl titanate are template and titanium source, respectively. The hydrothermal synthesis was performed in Teflon-lined autoclave and held at 443 K under stirring for 72 h. The product was cooled down to room temperature and centrifugated. The solid product was dried at 373 K for 12 h and then calcined at 813 K for 6 h. This final product is the home-made TiO_2.

2.2. Material characterization

The UV-Raman spectrum was recorded using a home-made triple stage UV-Raman spectrograph with exciting line of 244 nm, 257 nm, 266 nm and 325 nm. The high-resolution ^{1}H NMR spectrum was obtained on a Bruker AVANCE-III spectrometer. DFT calculation of Ti-sites in TS-1 catalysts are shown in Supporting Information. XRD pattern was obtained with a SmartLab(9) diffractometer using a CuK_α radiation operated at 40 kV and 100 mA. The N_2 physisorption isotherm was obtained at liquid nitrogen temperature using a Quantachrome Autosorb S1 physical sorption apparatus. The pore size distribution was obtained by the BJH method. The total surface area and pore volume were calculated using the BET and t-plot method, respectively. The transmission electron microscopy (TEM) image was taken on the HT7700 instrument (Hitachi High-Tech) with an acceleration voltage of 100 kV. The UV-Vis spectrum was obtained using a Jasco UV-550 spectrometer with pure $BaSO_4$ as reference. Inductively coupled plasma optical emission spectrometer (ICP-OES) was performed on PerkinElmer AVIO 500 optical emission spectrometer.

2.3. Quantification of Ti sites in TS-1 catalysts

The amounts of different Ti-sites in each catalyst were estimated from the ICP-OES data, UV-Raman spectrum and de-convoluted UV-Vis absorption bands of the catalyst by the following steps:

(i) The total Ti amount (Ti_{Total}/mol g^{-1}) of each TS-1 catalyst was calculated from the ICP-OES result;
(ii) Identify types of Ti sites within the catalyst by UV resonance Raman spectroscopy and suitable exciting lines to detect them;
(iii) Deconvolute the UV-Vis spectrum by Peakfit and results from step (ii) to isolate the peak for each identified Ti site;
(iv) Integrate each acquired peak by Origin so as to calculate the peak area, $A(Ti)_i$. It must be pointed out that only the right half of each acquired peak is integrated. This is due to instrumental limitation where the cut off for the UV-Vis spectrum was at 190 nm, resulting in incomplete peak at ~210 nm;
(v) Calculate the amount of each Ti site using the following formula:

$$n(Ti)_i=(A(Ti)_i/\sum A(Ti)_i)\times Ti_{Total}$$

2.4. Catalytic performance testing of materials

The catalytic performance of the TS-1 catalysts and two anatase-TiO_2 samples was evaluated by propylene epoxidation. 0.10 g TS-1 catalyst powder and 34 ML of 3.0 mol/L H_2O_2/methanol solution were firstly introduced into a 400 ML stainless steel reactor. Propylene was then charged into the reactor to reach 0.6 MPa pressure. The reaction was terminated after heating the mixture at 303 K for 10 min, 20 min, 30 min, 40 min, 50 min and 60 min, respectively.

0.20 g TiO_2 sample powder and 34 ML of 2.0 mol/L H_2O_2/methanol solution were firstly introduced into a 400 ML stainless steel reactor. Propylene was then charged into the reactor to reach 0.6 MPa pressure. The reaction was terminated after heating the mixture at 323 K for 60 min

The residual H_2O_2 was measured by iodometric titration. The reaction products were analyzed using a Tianmei 7890 F gas chromatograph equipped with a flame ionization detector (FID) and a PEG-20 m capillary column (30 m × 0.25 m×0.4 μm). Propylene oxide (PO) is the target product and propylene glycol (PG) and its monomethyl ethers (MME) are byproducts. The conversion of H_2O_2 ($X(H_2O_2)$), selectivity of PO (S(PO)), utility of H_2O_2 ($U(H_2O_2)$), yield of PO (Y(PO)) and conversion of propylene to PO ($X(C_3H_6)$) were calculated using formula (1) to (5), respectively. Here $n_o(H_2O_2)$ and $n(H_2O_2)$ are the initial and final molar number of H_2O_2, respectively; n(PO), n(MME) and n(PG) are the molar number of the PO, MME and PG, respectively.

$$X(H_2O_2)=1\text{-}n(H_2O_2)/n_o(H_2O_2) \quad (1)$$

$$S(PO)=n(PO)/(n(PO)+n(MME)+n(PG)) \quad (2)$$

$$U(H_2O_2)=(n(PO)+n(MME)+n(PG))/(n_o(H_2O_2)\times X(H_2O_2)) \quad (3)$$

$$Y(PO)=X(H_2O_2)\times S(PO)\times U(H_2O_2) \quad (4)$$

$$X(C_3H_6)= Y(PO) \quad (5)$$

3. Results and discussion

3.1. Ti-sites in TS-1 catalysts

UV resonance Raman spectroscopy with exciting line of 244 nm, 257 nm and 266 nm (λ_{ex}=244 nm, 257 nm and 266 nm) is used to detect the types of Ti-sites in T-TS-1 and ML-TS-1. Fig. 1 is the UV-Raman spectra of the two TS-1 catalysts. As seen, the Raman peaks at 380 cm^{-1} and 800 cm^{-1} associated with the MFI topology are clearly seen for all catalysts as expected. Additionally, the peaks at 960 cm^{-1} are also seen for all catalysts and it is attributed to the vibration of Si-O bonds [24]. The peak at 1125 cm^{-1} exists for all and it is assigned to Ti-O-Si bonds [7,25,26].

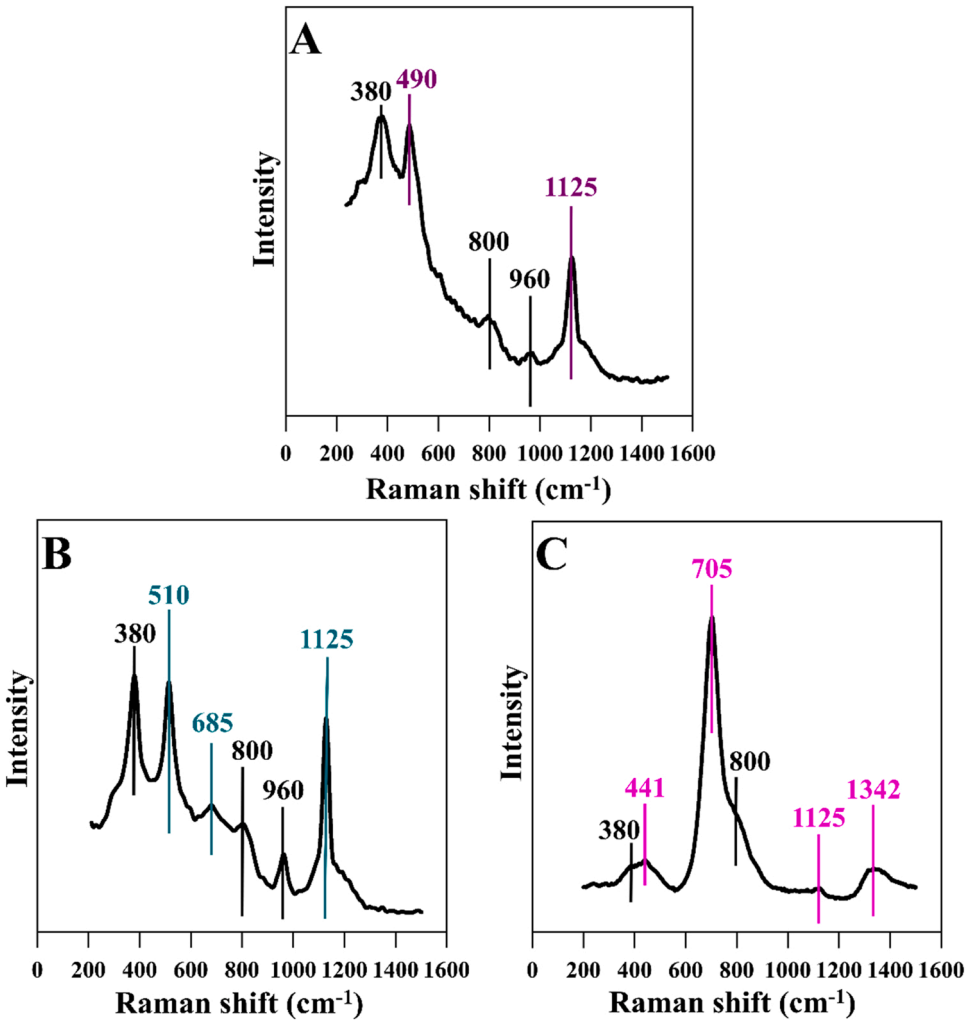

Fig. 1. UV-Raman spectra of T-TS-1 and ML-TS-1 catalysts. (A) UV-Raman spectrum excited at 244 nm of T-TS-1. (B) UV-Raman spectrum excited at 257 nm of T-TS-1. (C) UV-Raman spectrum excited at 266 nm of ML-TS-1.

Fig. 1 A is the UV-Raman spectrum of T-TS-1 excited at 244 nm. In addition to the ascribed peaks, it presents a peak at 490 cm^{-1}. As shown in our previous reports [7], the co-existence of the three peaks at 490, 530 and 1125 cm^{-1} on the 244 nm-excited Raman spectrum proves the existence of "TiO_4", a tetra-coordinated Ti site made of four Ti-O-Si bonds in the framework ($Ti(OSi)_4$). The Raman peak at 530 cm^{-1} attributed to "TiO_4" has disappeared completely, whilst the Raman peaks at 490 cm^{-1} and 1125 cm^{-1} remain. This suggests that the two peaks are likely associated to a "new" Ti-site in T-TS-1. Fig. 1B is the UV-Raman spectrum of T-TS-1 excited at 257 nm. There are two new peaks at 510 cm^{-1} and 685 cm^{-1} observed, indicating that there could be another "new" Ti-site in the T-TS-1 catalyst. Additionally, the 266 nm-excited UV-Raman spectrum of ML-TS-1 in Fig. 1C presents the three new peaks at 441, 705 and 1342 cm^{-1}. This indicates the existence of a third "new" Ti-site in ML-TS-1 catalyst.

So far, UV-Raman analysis indicates "new" Ti-sites exist in T-TS-1 and ML-TS-1. These "new" sites all contain Ti-O-Si bonds as the 1125 cm^{-1} peaks are shown on their Raman spectra. Their ^1H NMR results in Fig. S1 demonstrate that there are Ti-O-H bonds in the two catalysts. Density functional theory (DFT) calculations were carried out to confirm the assignments of the Raman peaks and to establish the coordination structures of the "new" Ti-sites in the three catalysts. The

Table 1
Assignment of experimental Raman peaks and coordination structures of Ti-IV, Ti-V and Ti-VI sites based on the DFT calculation.

Raman Peak (cm^{-1})		Raman peak assignment	Coordination structure			Ti-site
DFT calculated	Experimentally measured		Coordination number	Ti-O-Si bonds	Ti-O-H bond (s)	
493	490	Ti-O-Si bending	4	3	1	Ti-IV
1130	1125	Ti-O-Si stretching				
776	—	Ti-O-H stretching				
511	510	Ti-O-H wagging	5	3	2	Ti-V
680	685	Ti-O-H rocking				
1119	1125	Ti-O-Si stretching				
440	441	Ti-O-H wagging	6	2	4	Ti-VI
709	705	Ti-O-H rocking				
1119	1125	Ti-O-Si stretching				
1339	1342	Si-O-H rocking				

DFT calculated and experimentally observed Raman peaks are listed in Table 1.

As seen, the calculated Raman peaks match almost perfectly to the experimentally observed peaks for all three Ti-sites, confirming the coordination structures of the sites as presented in Table 1.

As stated previously, for the Ti-site detected by the 244 nm UV-Raman spectroscopy, the Raman peaks at 490 and 1125 cm^{-1} are due to the bending and stretching vibrations of its Ti-O-Si bonds, respectively. DFT also reveals an additional Raman peak at 776 cm^{-1} associated with the stretching of Ti-O-H bonds. This site is thus confirmed as a tetra-coordinated Ti-site containing three Ti-O-Si bonds and one Ti-O-H bond, and it is named Ti-IV ($TiOH(OSi)_3$). The coordination structure of this site was proposed before based on UV-Vis spectra result [24], and it is now experimentally observed by the UV resonance Raman spectroscopy in this work.

For the Ti-site detected by the 257 nm UV-Raman spectroscopy, the Raman peaks at 510 and 685 cm^{-1} are associated with the wagging and rocking vibrations of Ti-O-H bonds, respectively. The peak at 1125 cm^{-1} is due to the stretching vibration of Ti-O-Si bonds. This site is indeed a penta-coordinated Ti-site containing three Ti-O-Si bonds and two Ti-O-H bonds. This new Ti-site is named Ti-V ($Ti(OH)_2(OSi)_3$).

For the Ti-site detected by the 266 nm UV-Raman spectroscopy, the Raman peaks at 441 and 705 cm^{-1} are associated with the wagging and rocking vibrations of the Ti-O-H bonds, respectively. The peak at 1125 cm^{-1} is due to the stretching vibration of Ti-O-Si bonds. Finally, the peak at 1342 cm^{-1} is assigned to the rocking vibration of Si-O-H bonds. This is a hexa-coordinated Ti-site containing two Ti-O-Si bonds and four Ti-O-H bonds. This new Ti-site is named Ti-VI ($Ti(OH)_4(OSi)_2$). The proposed structures of the Ti-IV, Ti-V and Ti-VI are presentd in Fig. 2.

3.2. Catalytic activities of Ti-sites in TS-1 catalysts

In this study, catalytic activities of Ti-IV, Ti-V and Ti-VI are evaluated by the turnover frequency (TOF) determined in propylene (C_3H_6) epoxidation to propylene oxide (PO) over the T-TS-1 and ML-TS-1 catalysts. Moreover, m-TS-1 containing "TiO_4" and T*-TS-1 with the known hexa-coordinated "TiO_6" site ($Ti(OH_2)_2(OH)_2(OSi)_2$) (Fig. S2) are also evaluated to compare catalytic activities of the five Ti-sites. It is shown that "TiO_6" is made of two Ti-O-Si bonds, two Ti-O-H bonds and two H_2O molecules, and it is different from the new Ti-VI (Fig. S3).

Propylene conversion is used to evaluate the catalytic activity of the four catalysts and their Ti-sites. Fig. 3A shows the propylene conversion vs. reaction time ($X(C_3H_6)$-t) curves over the four catalsyts. As seen, propylene conversion of the four catalysts follows m-TS-1 <T-TS-1 <T*-TS-1 <ML-TS-1. They have progressively higher propylene conversion from 0 min to 60 min and the sharp increase in the first 10 min demonstrates a high initial reaction rate before slowing down. The TOF of each catalyst (TOF(Catalyst)) is thus calculated based on its propylene conversion within 0–10 min. The full details on TOF(Catalyst) determination are provided in Fig. S4 and Table S1. Fig. 3B presents the TOF (Catalyst) of the four catalysts, showing ML-TS-1 has the highest TOF value (thus the highest catalytic activity) of 5.44 mol $(g\ min)^{-1}$, which is about 1.4, 2.4 and 3.7 times higher than that of T*-TS-1, T-TS-1 and m-TS-1.

m-TS-1, T-TS-1, T*-TS-1 and ML-TS-1 have same MFI topology, similar morpology and particle size (Fig. S5 and Fig. S6). Moreover, the differences in catalytic activities are not attached to their pore size distribution, pore structure, surface area and pore volume of the four catalysts (Fig. S7, Fig. S8 and Table S2). Thus, the significantly enhanced catalytic activity observed of ML-TS-1 hints strongly the existence of more intrinsic differences in activity of Ti-sites in these catalysts. m-TS-1 contains only "TiO_4", but the other three TS-1 catalysts contain Ti-IV, Ti-V, "TiO_6", Ti-VI and anatase-TiO_2 (Fig. S2 and Fig. S9). For T-TS-1, T*-TS-1 and ML-TS-1, they all contain Ti-IV and Ti-V and anatase-TiO_2. The quantities of Ti-IV and Ti-V follow T-TS-1 >T*-TS-1 >ML-TS-1. The quantities of anatase-TiO_2 are similar in T-TS-1 and T*-TS-1, but both are higher than in ML-TS-1. In addition, T*-TS-1 also contains "TiO_6" and ML-TS-1 contains Ti-VI, although the quantities of the two sites are similar in the two catalysts (Table S3). Thus, effect of anatase-TiO_2 on propylene epoxidation is studied before calculating the TOFs of other Ti-sites.

Commercial anatase-TiO_2 and home-made anatase-TiO_2 were in this section to understand their effects on the propylene epoxidation. The UV-Raman resonance spectra (Fig. 3C) display the characteristic peaks of anatase-TiO_2 (144, 390, 515 and 637 cm^{-1} [12]) for both the commercial and home-made anatase-TiO_2 samples. As shown in Fig. 3D, no propylene converts because no PO and other byproducts generate. However, "H_2O_2 conversion ($X(H_2O_2)$)" is 2.6%, implying the "conversion" is the decomposition of H_2O_2 caused by the home-made TiO_2. No reaction was observed over the commercial anatase-TiO_2. These results demonstrate that the anatase-TiO_2 has no activity in the propylene epoxidation. Effect of anatase-TiO_2 on H_2O_2 conversion can be ignored because its amounts in TS-1 catalysts are extremely low (Table S3).

TOFs of Ti-VI, "TiO_6", Ti-IV+Ti-V and "TiO_4" sites ($TOF(Ti\text{-}site)_i$) in the four TS-1 catalysts were calculated by the amount of each type of Ti site ($n(Ti\text{-}site)_i$) in Table S3 and TOF(Catalyst) in Fig. 3B through the following formula. The details to calculate TOF of Ti-sites are shown in S8, Supporting Information.

$$TOF(Catalyst)=\sum[TOF(Ti\text{-}site)_i \times n(Ti\text{-}site)_i]$$

Fig. 3E presents $TOF(Ti\text{-}site)_i$ for the Ti-VI, "TiO_6", Ti-IV+Ti-V and

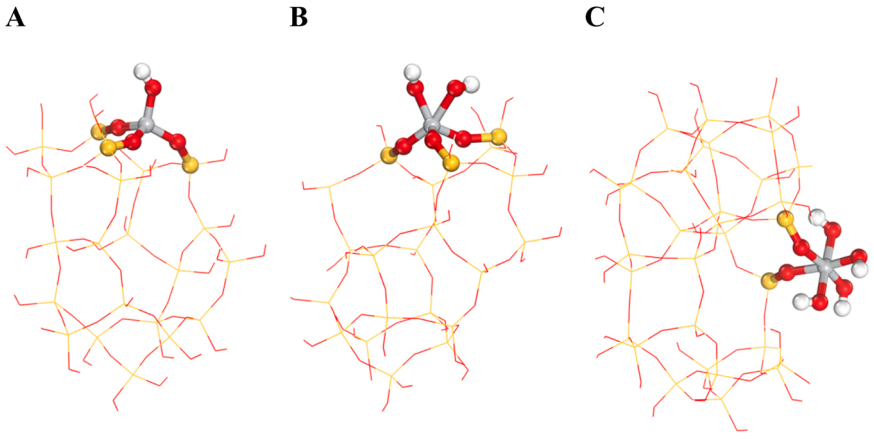

Fig. 2. Proposed structures of the Ti-IV(A), Ti-V (B) and Ti-VI (C) by DFT. The grey ball represents the Ti atom, yellow for Si, red for O and white for H. They are the results after geometric optimization and frequency calculations.

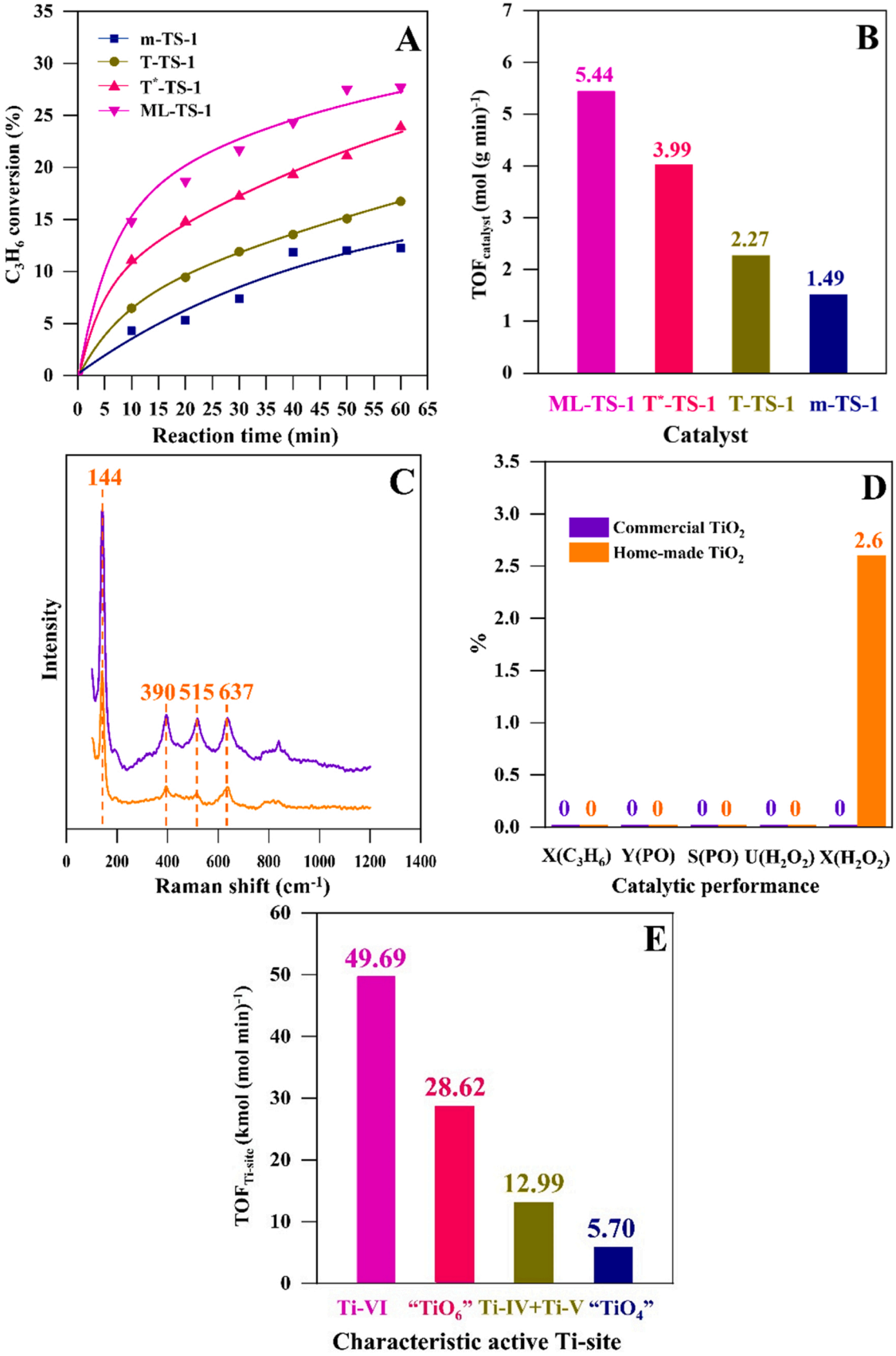

Fig. 3. Catalytic activities of TS-1 catalysts and Ti-sites. (A) Propylene conversion vs. reaction time (X(C_3H_6)-t) curves of m-TS-1, T-TS-1, T*-TS-1 and ML-TS-1. (B) Turnover frequency (TOF) of the four catalysts. (C) UV-Raman resonance spectra (λ_{ex}=325 nm) of commercial anatase-TiO_2 and home-made anatase-TiO_2. (D) Catalytic performance of commercial TiO_2 and home-made TiO_2. (E) TOF of the characteristic active Ti-sites in these catalysts.

"TiO_4" sites. Obviously as seen in the figure, Ti-VI has an exceptionally high TOF under the reaction conditions studied. It has a TOF of 49.69 kmol (mol min)$^{-1}$, ~1.7, 3.8 and 8.7 times that of "TiO_6", Ti-IV+Ti-V and "TiO_4", respectively. Higher TOF of Ti-VI than the other Ti-sites indicates that Ti-VI also has better catalytic ability to activate H_2O_2 in propylene epoxidation than "TiO_6", Ti-IV+Ti-V and "TiO_4". It is, therefore, concluded that the existence of Ti-VI is the primary reason for the observed higher catalytic activity of ML-TS-1.

As m-TS-1, T-TS-1, T*-TS-1 and ML-TS-1 have almost same propylene oxide selectivity (S(PO) = 98.6%− 99.5%, Table S4) and H_2O_2 utility (U(H_2O_2) = 97.9%− 100.0%, Table S5), differences in types and amounts of Ti-sites in the four catalysts have minor effects on S(PO) and U(H_2O_2). Besides, ML-TS-1 demonstrates a sustained activity (250 h) with propylene oxide selectivity and H_2O_2 conversion of ~ 98% and 95%, respectively after 250 h time-on-stream (Fig. S10).

4. Conclusions

In conclusion, two new Ti-sites, including the penta-coordinated Ti $(OH)_2(OSi)_3$ (Ti-V) and hexa-coordinated $Ti(OH)_4(OSi)_2$ (Ti-VI) in TS-1 catalysts are created. Ti-V and Ti-VI are identified by UV resonance Raman spectroscopy. Characteristic Raman peaks of Ti-V are at 510, 685 and 1125 cm^{-1}. For Ti-VI, they are at 441, 705, 1125 and 1342 cm^{-1}. The catalytic activity of Ti-VI is ~1.7, 3.8 and 8.7 times the activity of "TiO_6", Ti-IV+Ti-V and "TiO_4", respectively in propylene epoxidation to propylene oxide. Ti-VI is determined to be highly active Ti-site for propylene epoxidation.

CRediT authorship contribution statement

Yanli Wang: material preparation, characterization, catalytic tests, TOF study, original draft. **Hong Yang:** Writing-review & design & editing. **Yi Zuo:** TOF study. **Dongxu Tian, Yaqiong Su:** DFT study. **Guangjin Hou:** ^{1}H NMR analysis. **Zhaochi Feng:** UV-Raman analysis and structure investigation. **Xinwen Guo, Can Li:** Designing study, experiments and paper.

Data Availability

Data will be made available on request.

Acknowledgements

We thank Professor Chunshan Song for suggestions to paper writing and Doctor Haiyan Wang for giving suggestions to calculate TOFs. This work is financially supported by Fundamental Research Center of Artificial Photosynthesis (FReCAP), National Natural Science Foundation of China (NSFC) 22272163, Liaoning Revitalization Talent Program (XLYC2008032), Fundamental Research Fundamental Funds for the Central Universities (DUT22LAB602).

Declaration of competing interests

Authors declare that they have no competing interests.

Appendix A. Supporting information

Supplementary data associated with this article can be found in the online version at doi:10.1016/j.apcatb.2023.122396.

References

[1] M. Taramasso, G. Perego, B. Notari, Preparation of porous crystalline synthetic material comprised of silicon and titanium Oxides, U.S. Patent ,1983 No. 4410501.
[2] D.R.C. Huybrechts, L. De Bruycker, P.A. Jacobs, Oxyfunctionalization of alkanes with hydrogen peroxide on titanium silicalite, Nature 345 (1990) 240–242.
[3] P.T. Tanev, M. Chlbwe, T.J. Plnnavala, Titanium-containing mesoporous molecular sieves for catalytic oxidation of aromatic compounds, Nature 368 (1994) 321–323.
[4] S. Saxena, J. Basak, N. Hardia, R. Dixit, S. Bhadauria, R. Dwivedi, R. Prasad, A. Soni, G.S. Okram, A. Gupta, Ammoximation of cyclohexanone over nanoporous TS-1 using UHP as an oxidant, Chem. Eng. J. 132 (2007) 61–66.
[5] Z.H. Zhang, Y.Q. Tang, W. Du, J.L. Xu, Q.H. Wang, N. Song, G. Qian, X.Z. Duan, X. G. Zhou, Engineering gold impregnated uncalcined TS-1 to boost catalytic formation of propylene oxide, Appl. Catal. B 319 (2022) 121837–121849.
[6] M. Lin, C.J. Xia, B. Zhu, H. Li, X.T. Shu, Green and efficient epoxidation of propylene with hydrogen peroxide (HPPO process) catalyzed by hollow TS-1 zeolite: a 1.0 kt/a pilot-scale study, Chem. Eng. J. 295 (2016) 370–375.
[7] C. Li, G. Xiong, Q. Xin, J.K. Liu, P.L. Ying, Z.C. Feng, J. Li, W.B. Yang, Y.Z. Wang, G. R. Wang, X.Y. Liu, M. Lin, X.Q. Wang, E.Z. Min, UV resonance Raman spectroscopic identification of titanium atoms in the framework of TS-1 zeolite, Angew. Chem. Int. Ed. 38 (1999) 2220–2222.
[8] C.P. Gordon, H. Engler, A.S. Tragl, M. Plodinec, T. Lunkenbein, A. Berkessel, J. H. Teles, A.N. Parvulescu, C. Copéret, Efficient epoxidation over dinuclear sites in titanium silicalite-1, Nature 586 (2020) 708–713.
[9] Q. Guo, K.Q. Sun, Z.C. Feng, G.N. Li, M.L. Guo, F.T. Fan, C. Li, A thorough investigation of the active titanium species in TS-1 zeolite by in situ UV resonance Raman spectroscopy, Chem. Eur. J. 18 (2012) 13854–13860.
[10] W.J. Xu, T.J. Zhang, R.S. Bai, P. Zhang, J.H. Yu, A one-step rapid synthesis of TS-1 zeolites with highly catalytically active mononuclear TiO_6 species, J. Mater. Chem. A 8 (2020) 9677–9683.
[11] L.Z. Wu, X.J. Deng, S.F. Zhao, H.M. Yin, Z.X. Zhuo, X.Q. Fang, Y.M. Liu, M.Y. He, Synthesis of a highly active oxidation catalyst with improved distribution of titanium coordination states, Chem. Commun. 52 (2016) 8679–8682.
[12] G. Xiong, Y.Y. Cao, Z.D. Guo, Q.Y. Jia, F.P. Tian, L.P. Liu, The roles of different titanium species in TS-1 zeolite in propylene epoxidation studied by in situ UV Raman spectroscopy, Phys. Chem. Chem. Phys. 18 (2016) 190–196.
[13] M. Signorile, L. Braglia, V. Crocell, P. Torelli, E. Groppo, G. Ricchiardi, S. Bordiga, F. Bonino, Titanium defective sites in TS-1: structural insights by combining spectroscopy and simulation, Angew. Chem. Int. Ed. 59 (2020) 18145–18150.
[14] W.B. Fan, R.G. Duan, T. Yokoi, P. Wu, Y. Kubota, T. Tatsumi, Synthesis, crystallization mechanism, and catalytic properties of titanium-rich TS-1 free of extraframework titanium species, J. Am. Chem. Soc. 130 (2008) 10150–10164.
[15] N.A. Grosso-Giordano, A.S. Hoffman, A. Boubnov, D.W. Small, S.R. Bare, S.I. Zones, A. Katz, Dynamic reorganization and confinement of Ti^{IV} active sites controls olefin epoxidation catalysis on two-dimensional Zeotypes, J. Am. Chem. Soc. 141 (2019) 7090–7106.
[16] W.O. Parker, R. Millini, Ti coordination in titanium silicalite-1, J. Am. Chem. Soc. 128 (2006) 1450–1451.
[17] Y. Zuo, M. Liu, T. Zhang, C.G. Meng, X.W. Guo, C.S. Song, Enhanced catalytic performance of titanium silicalite-1 in tuning the crystal size in the range 1200–200 nm in a tetrapropylammonium bromide system, ChemCatChem 7 (2015) 2660–2668.
[18] M. Liu, Z.H. Chang, H.J. Wei, B.J. Li, X.Y. Wang, Y.Q. Wen, Low-cost synthesis of size-controlled TS-1 by using suspended seeds: from screening to scale-up, Appl. Catal. A Gen. 525 (2016) 59–67.
[19] J. Shi, Y. Wang, W. Yang, Y. Tang, Z. Xie, Recent advances of pore system construction in zeolite-catalyzed chemical industry processes, Chem. Soc. Rev. 44 (2015) 8877–8903.
[20] Y. Wei, T.E. Parmentier, K.P. de Jong, J. Zečevic, Tailoring and visualizing the pore architecture of hierarchical zeolites, Chem. Soc. Rev. 44 (2015) 7234–7261.
[21] X.B. Wang, M.Y. Sun, B. Meng, N.T. Yang, S.J. Zhuang, X.Y. Tan, S.M. Liu, Influence of silicalite-1 nanoparticle seeds on the synthesis of Ti-containing mesoporous zeolites, Chem. Eng. J. 289 (2016) 494–501.
[22] L.H. Chen, X.Y. Li, G. Tian, Y. Li, J.C. Rooke, G.S. Zhu, S.L. Qiu, X.Y. Yang, B.L. Su, Highly stable and reusable multimodal zeolite TS-1 based catalysts with hierarchically interconnected three-level micro-meso-macroporous structure, Angew. Chem. Int. Ed. 123 (2011) 11352–11357.
[23] N. Wilde, M. Pelz, S.G. Gebhardt, R. Gläser, Highly efficient nano-sized TS-1 with micro-/mesoporosity from desilication and recrystallization for the epoxidation of biodiesel with H_2O_2, Green Chem. 17 (2015) 3378–3389.
[24] P. Ratnasamy, D. Srinivas, H. Knozinger, Active sites and reactive intermediates in titanium silicate molecular sieves, Adv. Catal. 48 (2004) 1–169.
[25] F.T. Fan, Z.C. Feng, C. Li, U.V. Raman spectroscopic studies on active sites and synthesis mechanisms of transition metal containing microporous and mesoporous materials, Acc. Chem. Res. 43 (2010) 378–387.
[26] F.T. Fan, Z.C. Feng, C. Li, In-situ characterization of heterogeneous catalysts themed issue, Chem. Soc. Rev. 39 (2010) 4794–4801.